Groundwater for Sustainable Development 25 (2024) 101188

Contents lists available at ScienceDirect

Groundwater for Sustainable Development

journal homepage: www.elsevier.com/locate/gsd

Research paper

Innovative mapping of groundwater redox status and cation exchange conditions in a GIS environment

Mojtaba Zaresefat [a,*], Walter Schenkeveld [b], Reza Derakhshani [c,d], Jasper Griffioen [a,e]

[a] Copernicus Institute of Sustainable Development, Utrecht University, Utrecht, the Netherlands
[b] Soil Chemistry and Chemical Soil Quality, Wageningen University and Research, Wageningen, the Netherlands
[c] Department of Earth Sciences, Utrecht University, Utrecht, the Netherlands
[d] Department of Geology, Shahid Bahonar University of Kerman, Kerman, Iran
[e] TNO Geological Survey of the Netherlands, Utrecht, the Netherlands

HIGHLIGHTS

- The method employs Empirical Bayesian Kriging and the Math toolbox in ArcMap in a two-step approach.
- The method was tested in the coastal lowlands of the western Netherlands.
- The method produced a 75%–95% agreement between predicted and observed groundwater status, proving its effectiveness.
- The method was simpler and straightforward compared to other approaches for mapping non-numeric hydrogeochemical classes.

GRAPHICAL ABSTRACT

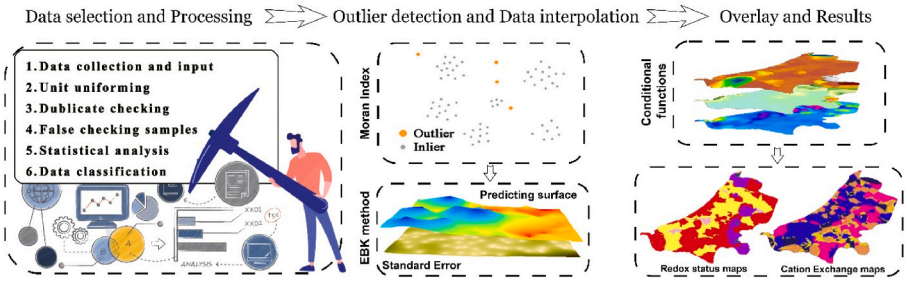

ARTICLE INFO

Keywords:
Groundwater monitoring
Cartography
Non-numerical indices
Geostatistics
Conditional functions
ArcGIS

ABSTRACT

Understanding the complexities of regional groundwater quality is crucial for managing groundwater resources. Groundwater quality assessment involves investigating specific dissolved groundwater components, for example, comparing them to established standards. To fully understand all aspects of groundwater quality, one should assess composite properties, one being the redox status and another being the cation exchange condition. The first may, for example, impose a control on the degradation of organic micropollutants. While groundwater numerical indices can be easily interpolated and visualised using various GIS applications, consistently mapping the redox status and cation exchange conditions as non-numerical indices remains challenging. Furthermore, no study has yet conducted a regional-scale mapping of cation exchange classes in a GIS environment using extensive groundwater samples. To deepen our understanding of these groundwater components, we employed ArcGIS in this study to map the redox and cation exchange conditions in two stages. First, we mapped the groundwater components of interest, including Cl, SO_4, SO_4/Cl, Fe, NO_3 and base exchanges of Na and Mg, by the most appropriate interpolation method identified by a geostatistical analysis. Then, variables were combined, and the conditional functions were used in ArcMap's Math toolbox to determine redox status or cation exchange classes. Our innovative GIS method for mapping regional redox status and cation exchange conditions was developed for 3350 groundwater sampling locations in the coastal lowlands of the Western Netherlands. The method was successful, with generally 75%–95% similarity between predicted and observed situations for most

* Corresponding author.
E-mail address: m.zaresefat@uu.nl (M. Zaresefat).

https://doi.org/10.1016/j.gsd.2024.101188
Received 14 November 2023; Received in revised form 24 April 2024; Accepted 25 April 2024
Available online 26 April 2024

classes. The introduced method is more straightforward than others and can map other non-numerical linguistic indices like Wilcox groundwater and irrigation water classifications, as well.

1. Introduction

Groundwater accounts for approximately 50% of the world's drinking water, 40% of irrigation water and 30% of industrial water (Lall et al., 2020). Groundwater resource quality is often affected by human activities such as industrialisation, agriculture and natural processes, including redox reactions and cation exchange. Understanding regional-scale groundwater quality is essential to managing groundwater resources and evaluating risks to the drinking water supply, among others (Ehteshami et al., 2016).

Groundwater quality status can be evaluated by assessing specific dissolved species concentrations and comparing them to accepted standards (e.g., for drinking water). Alternatively, when compared with the mineral solubility constant, certain quality parameters are calculated as the sum of solute concentrations (e.g., the salinity) or as product (e.g., the ion activity product). These characteristics are numerical and are based on multiple solutes. There are also non-numerical classes, such as groundwater's redox status, a commonly considered quality parameter. Based on the presence or absence of redox-sensitive solutes, groundwater can be characterised by redox classes such as 'anoxic' (Appelo and Postma, 2004; Drever, 1997). Although the redox potential of groundwater could be considered a numerical parameter indicative of the redox status, this parameter is usually determined by one dominant redox couple that is not necessarily in equilibrium with other active redox couples (Søndergaard, 2009). In other words, the value of the redox potential depends on which redox couple is measured. As a result of this dependency, characterisation of the redox status by classes is often preferred.

Another non-numerical class of groundwater quality is the cation exchange status. Cation exchange with the sorption complex induces shifts in concentration due to the exchange between adsorbed and dissolved cations such as Na^{+} and Ca^{2+}. The cation exchange process is particularly relevant in coastal aquifers, where aquifer salinisation (displacement of fresh groundwater by saline groundwater) or freshening (displacement of saline groundwater by fresh groundwater) occurs (Appelo and Postma, 2004; Naus et al., 2019). Here, the extent of salinisation or freshening can be expressed quantitatively, thereby demonstrating the composition of infiltrating water (Griffioen, 2003). One way to achieve this quantitative expression is via the Base Exchange Index (BEX) concept introduced by Stuyfzand (2008) to distinguish whether an aquifer is undergoing salinisation or freshening. However, the BEX does not account for temporal variations such as the initial or later stages of the cation exchange process. Furthermore, BEX application to different groundwater bodies should be done cautiously to avoid false-positive or false-negative results.

Obtaining a more detailed spatial understanding of the redox status and cation exchange conditions is essential to comprehend groundwater quality and its biogeochemical regulators, including the degradation of organic micropollutants. The redox status indicates which redox couples (such as sulphate/sulphide) may be active, thereby defining the degradation conditions for these micropollutants as well as their environmental impact (Christensen et al., 2000; Luo et al., 2014). However, the high spatial variability of base exchange indices and components of interest used to identify classes has made it challenging to determine the specific subgroup associated with salinisation/freshening processes or redox classification at the regional scale.

Due to this challenge, studies that estimate and map the redox status or act of cation exchange are rare but vital. Close et al. (2016) and Wilson et al. (2018) predicted the redox classes for the Waikato and Canterbury regions in New Zealand using Linear Discriminant Analysis (LDA). They compared the predicted redox status with those statuses which were assigned from groundwater analyses and found a strong correlation between them. Wolters et al. (2022) presented a methodology for mapping denitrification in groundwater based on a rank-based approach that makes use of the following: spatial, petrographic and hydrodynamic data on aquifer typologies in Germany; five commonly measured groundwater components; and a deterministic interpolation method. Additionally, Friedel et al. (2020) predicted the groundwater redox status in three regions of New Zealand. They showed that, compared with the three commonly used supervised learning-based methods of Random Forest (RF), Boosted Regression Tree (BRT) and LDA, their unsupervised learning-based method generated statistically significantly better correlations between measured and predicted values. All of the aforementioned studies considered point data and mapped the redox classes for unsampled areas. To our knowledge, no studies have mapped the cation exchange groups with extensive groundwater samples at the regional scale.

All groundwater quality data comes from existing or abandoned wells. Installing groundwater wells can be costly, and in many areas, this cost limits the spatial density of groundwater quality data. Hence, considerable uncertainty exists regarding the spatial and temporal distribution of redox and cation exchange zoning, an uncertainty which is amplified when data is interpolated. The level of uncertainty increases even more when data is extrapolated across larger geographical areas or becomes more complex due to variations in geological formations, landscapes, or land uses that impact groundwater composition.

Geographic Information Systems (GIS) provide a versatile environment for gathering, storing and presenting groundwater quality data for geospatial analysis and using these data to produce maps (Karimzadeh Motlagh et al., 2023). For example, the Thiessen polygons tool is a common GIS approach to visualise non-numerical values and extrapolate or generalise those values to areas without data. However, the use of this method faces several theoretical and practical constraints (Mu, 2009), the most important of which is inadequate consideration of spatial relationships among points. Two additional restrictions are that the method does not weigh the individual groundwater records and the method is entirely dependent on the sampling location.

This study addresses the challenge of mapping non-numerical groundwater quality data using readily available information. We propose a novel GIS method leveraging spatial relationships between multiple solute concentrations to classify groundwater composition. The method is developed and tested using data from the coastal lowlands of the Western Netherlands, demonstrating the method's applicability to diverse hydrogeological settings. While this region provides methodological context, the primary objective is not to conduct an exhaustive analysis of groundwater quality but to introduce and validate a broadly applicable approach for researchers and practitioners working in various geographic areas. We will therefore provide a concise description of the test region, prioritising the method's development, functionality and potential for wider implementation.

2. Test region and methods

To achieve a more accurate understanding of the spatial relationship between sample values and to extend this knowledge to other locations, the study conducted by Amini et al. (2019), Brindha et al. (2023) and Zaresefat et al. (2023b) emphasised the crucial role of employing the most suitable interpolation method. Building on this premise, we undertook a comprehensive geostatistical analysis to map all relevant solutes. To assess the redox status and cation exchange classes effectively, we integrated the generated maps, utilising conditional functions to determine the presence or absence of solutes or by comparing their

values. Below, we describe the procedure for our novel method, which allows us to identify spatial patterns of classes based on the underlying solute distributions method.

2.1. Test region

The test region lies at the southeastern border of the North Sea sedimentary basin (11,100 km^2). On average, the Netherlands has a temperate maritime climate with 887 mm/y of precipitation and 559 mm/y of potential evaporation (CLO, 2021). Approximately 60% of the area is a polder landscape, where the land surface is typically approximately two to 5 m below sea level. The groundwater basin in the Netherlands is wedge-shaped and increases in thickness from approximately 50 m in the ESE to 400–500 m in the WNW (Dufour, 2000). The study area's aquifer system comprises Holocene (marine, fluvial, aeolian) and Pleistocene (fluvial, marine and glacial) deposits and regional occurrences of Holocene peat. The groundwater is fresh to saline and suboxic to methanogenic (Griffioen et al., 2008, 2013). This region's geological and hydrological characteristics yield remarkable stability in groundwater properties; for example, groundwater that has remained unchanged for 4000 to 5000 years is common (Griffioen et al., 2013; Post et al., 2003; Van Geel et al., 2017).

The western edge borders the North Sea and mainly comprises a Holocene coastal dune belt approximately 150 km long and 8 km wide. Higher ice-pushed ridges form the area's eastern border. The deltaic Rhine River system flows through the southern part of the study area, and the Meuse River forms the area's southern border (Fig. 1).

The groundwater recharge is small in the test region due to the interception of infiltrating rain by shallow drainage, the poor permeability of the semi-confining top layer and the hydrological management

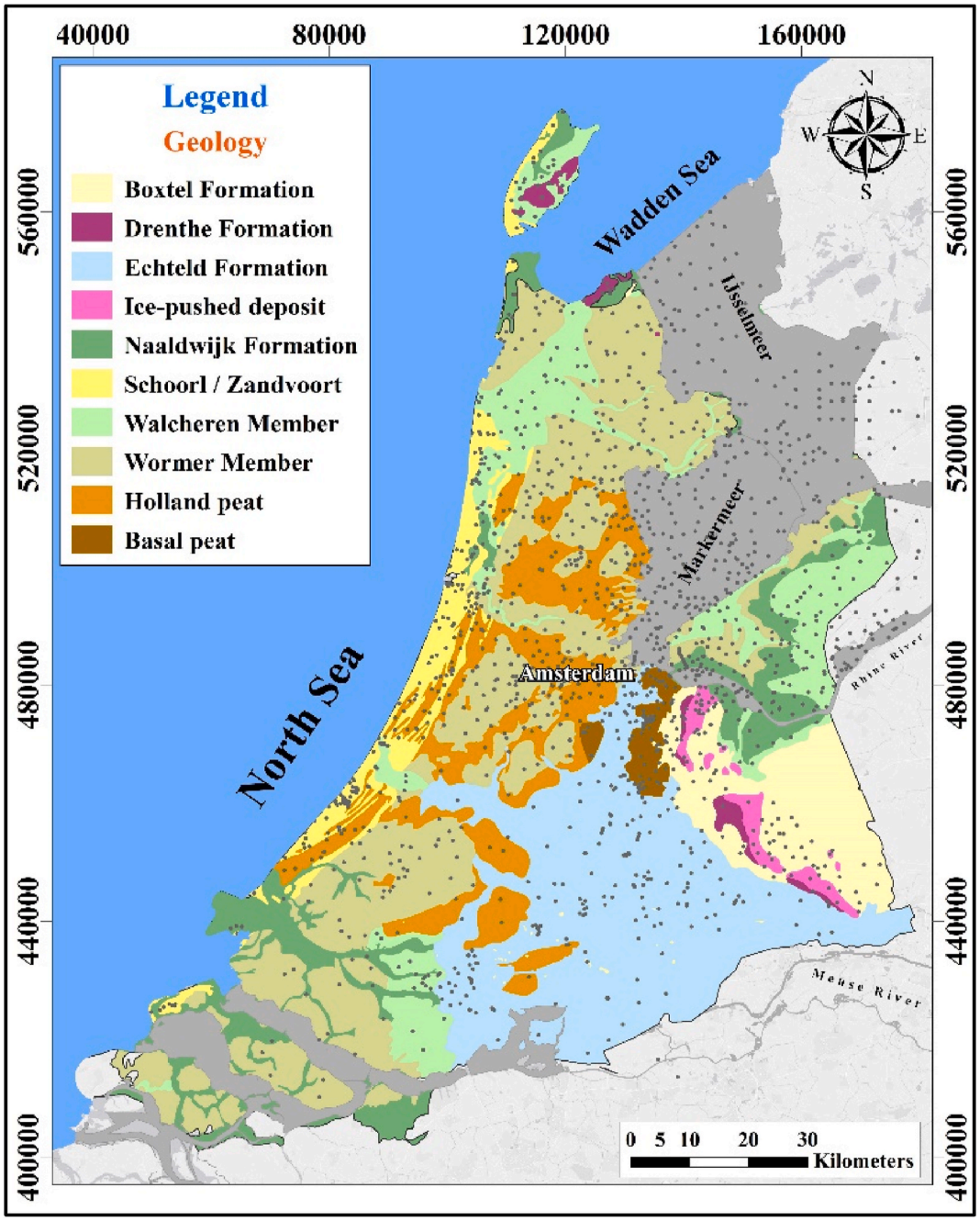

Fig. 1. *The surface geology of the test region, modified from* Weerts et al. (2006). *The locations of the groundwater wells are presented, as well.*

of the dune aquifer systems for drinking water supply. As is the case in many other coastal aquifers, salinisation and freshening are active hydrogeological processes in the study area (Appelo and Willemsen, 1987; Beekman, 1991; Griffioen, 1994). Consequently, dissolved cations are subject to cation exchange, especially because fresh, brackish and saline groundwaters are displaced relative to each other (Griffioen et al., 2013; Van Den Brink et al., 2007).

2.2. Methodology

Spatial Analyst and Math Toolbox in ArcMap are powerful features for spatial analysis and data modelling. These toolsets can automate multiple analysis steps in geoprocessing workflows using Python scripts or map algebra expressions. Raster and feature data tools abound in the Spatial Analyst toolbar. Utilising math functions to affect input values enables the conditional toolset to manipulate output values. The distance toolset allows straight-line or weighted distance analysis. Raster Math tools perform arithmetic, bitwise, logical and trigonometric operations on input rasters. For instance, the Divide tool divides two rasters cell-by-cell, while the Minus tool subtracts one raster (Esri, 2019).

In this study, each thematic map was prepared in three stages. First, all solute indicators required for classification were established using the information in the literature (Griffioen, 2003; Griffioen et al., 2013; Naus et al., 2019; Stuyfzand, 2008). Next, the necessary calculations for attributing a classification to a sample were performed. Finally, the map was prepared using conditional functions in the Raster Math toolset in ArcMap environments based on the overlay technique. ArcMap can predict or label the areas based on a given cell's value and the conditional statement. The Con tool was used to define the conditional statement and find the hydrogeochemical classes from the conditional input raster. We could easily control the output value for each cell based on whether the cell value was evaluated as true or false in a specified conditional statement using Con tools rather than other logical tools found in ArcMap's Math toolbox, such as Pick and SetNull. Fig. 2 is a schematic flowchart for mapping the redox and cation exchange conditions for eight depth intervals.

2.3. Data collecting and processing

Groundwater quality data from approximately 16,500 groundwater records collected from 1970 until 2010, consisting of major, minor and some trace constituents of groundwater, to a depth of 50 m below NAP (Amsterdam Ordnance Datum; Normaal Amsterdams Peil in Dutch) were compiled from the national database of TNO (Netherlands Organisation for Applied Scientific Research) and other sources. The concentration units were standardised, and checks were performed for duplicate entries, improbable combinations of parameter values (e.g., unusually low alkalinity at neutral pH) and improbable solute concentrations in relation to depth below NAP (e.g., high nitrate concentration at considerable depth), which led to 868 records being excluded. The electroneutrality condition was calculated (Equ. 1) using Phreeqc (Parkhurst and Appelo, 1999):

$$\frac{\sum(\text{equivalent of cations}) - \sum(\text{equivalent of anions})}{\sum(\text{equivalent of cations}) + \sum(\text{equivalent of anions})} \times 100 \quad (1)$$

The 4565 records that did not meet the criterion of the absolute value of the error percentage ≤10% were excluded. We then selected the groundwater components of interest, including Cl, Na, Mg, SO_4, Fe and NO_3, from the final database and calculated the SO_4/Cl ratio needed for redox classification and cation exchange classes (refer to Tables 1 and 2). Subsequently, the groundwater records of the database were divided into eight horizontal layers to reflect the overall horizontal layering of the aquifers as a quasi-3D model. The reasons for not using a full 3D model are illustrated in Zaresefat and Derakhshani, 2024. Ultimately, we calculated median values using SPSS if data from several samples (collected at different times) were present for a single screen (6678 analyses). Instead of average values, median values were used to minimise the impact of outliers due to analytical and other errors. We were left with 3350 groundwater compositions from 1875 wells (some of which had multiple screens).

Table 1
Criteria for the redox classification.

Redox class	NO_3 (mg/L)	Fe(mg/L)	SO_4/Cl (weight ratio)	SO_4(mg/L)
Suboxic	≥1.5	≤0.25		
Mixed	≥1.5	>0.25		
Fe anoxic	<1.5		≥0.128	
SO_4 reducing	<1.5		<0.128	≥1
SO_4 reduced	<1.5		<0.128	<1

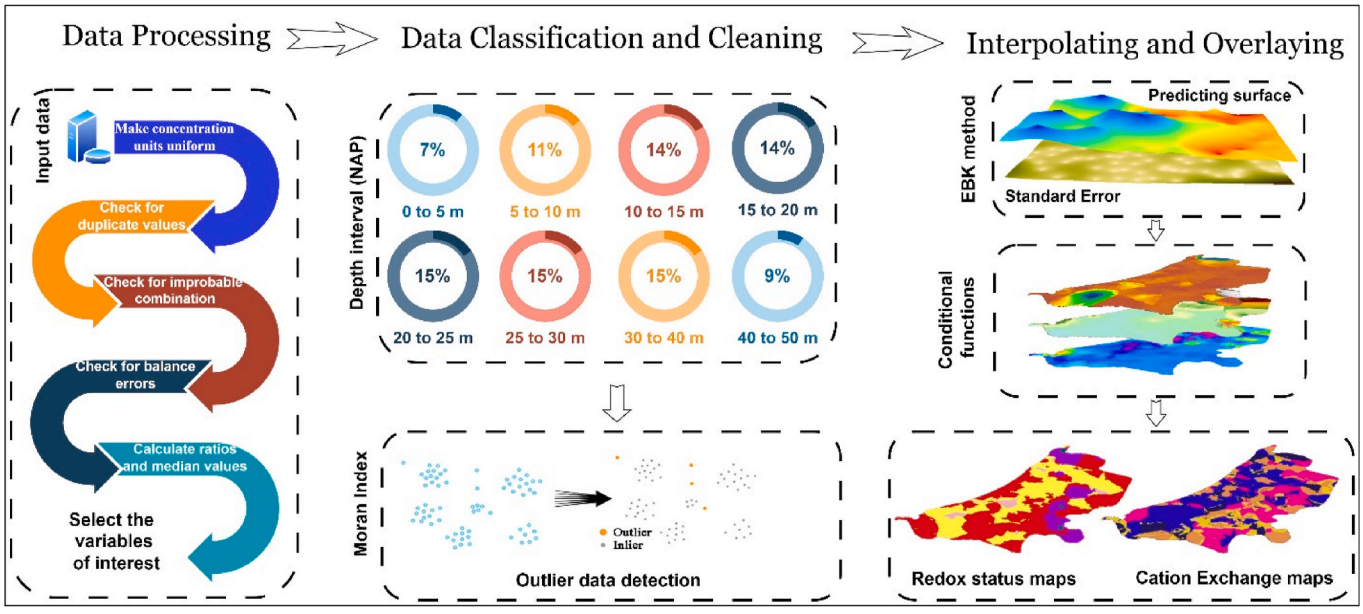

Fig. 2. Schematic flowchart outlining the mapping of redox status and cation exchange conditions using Math tools. EBK refers to Empirical Bayesian Kriging. The percentages illustrate the distribution of water samples across various depth intervals.

Table 2
The cation exchange classes.

No	Cation exchange group	Na-EXCH (meq/l)	Mg-EXCH (meq/l)	Cl (mg/L)
1	Late-stage of freshening – fresh water	>0.1	>0	<300
2	Late-stage of freshening – brackish water	>0.4	>0	300 < Cl < 5000
3	Late-stage of freshening – saline water	>0.15	>0	>5000
7	Initial freshening – fresh water	>0.1	<0	<300
8	Initial freshening – brackish water	>0.4	<0	300 < Cl < 5000
9	Initial freshening – saline water	>0.15	<0	>5000
10	No cation exchange	−0.1≤ ΔNa≥0.1		<300
		−0.4≤ ΔNa≥0.4		300 < Cl < 5000
		−1.5≤ ΔNa≥1.5		>5000
11	Initial salinising – fresh water	<-0.1	>0	<300
12	Initial salinising – brackish water	<-0.4	>0	300 < Cl < 5000
13	Initial salinising – saline water	<-0.15	>0	>5000
17	Late-stage of salinising – fresh water	<-0.1	<0	<300
18	Late-stage of salinising - brackish water	<-0.4	<0	300 < Cl < 5000
19	Late-stage of salinising – saline water	<-0.15	<0	>5000

2.4. Dataset classification

As mentioned above, redox status and cation exchange conditions are two important groundwater properties that control environmental geochemistry. Good maps are needed as a proper interpretation tool to identify transitions in redox or cation exchange conditions and their underlying causes to manage complex aquifer systems better. Groundwater compositions may change over time, but their redox status and cation exchange conditions will not change at the same speed (Griffioen et al., 2013).

2.4.1. Redox classes

Griffioen et al. (2013) devised a method for classifying the redox state of groundwater. Data on dissolved oxygen, CH_4 and H_2S concentrations were rarely available in our dataset, so these variables were not included as criteria to define the redox class. Table 1 presents the criteria we used. Samples were classified into five redox classes: 1) suboxic, 2) mixed, 3) Fe anoxic, 4) SO_4 reducing and 5) SO_4 reduced/methanogenic. For Dutch groundwater conditions, the SO_4 to Cl ratio is generally a valuable indicator of anthropogenic activities and SO_4 reduction for a combination of two reasons (Griffioen et al., 2013). One, there are no subsurface sources of Cl at shallow depths, such as rock salt dissolution or reductive dehalogenation. Two, gypsum is uncommon in Dutch Quaternary formations except in some marine clay soils due to oxic pyrite oxidation and pH-buffering by Ca carbonate dissolution. To assess groundwater records, the seawater SO_4 to Cl ratio serves as a reference for mixing between rain or river water and seawater (Griffioen et al., 2013; Pit et al., 2018): values above the reference ratio can be attributed to anthropogenic contamination and values below to SO_4 reduction. In the Rhine-Meuse delta, natural enrichment with SO_4 is common, partly due to riverbank infiltration of Rhine water with an SO_4 to Cl ratio above the seawater ratio (Griffioen et al., 2008). Due to Dutch groundwater's slightly acidic to slightly alkaline pH, dissolved iron typically exists in its ferrous (Fe(II)) form. The presence of both Fe(II) and nitrate here likely stems from two main causes: 1) mixing of shallow, nitrate-rich groundwater with deeper groundwater containing Fe(II) or 2) non-ideal redox behaviour within the aquifer.

2.4.2. Cation exchange classes

Cation exchange is expected in the test region due to fresh, brackish, and saline groundwater co-occurrence. The occurrence of cation exchange was assessed for each sample by calculating the enrichment or depletion of the cations compared with conservative mixing. The chloride concentration indicated the degree of conservative mixing between seawater and river or rainwater as end members. The degree of cation exchange was calculated as the deviation from a conservative concentration resulting from the mixing of the end members seawater and old River Rhine water as freshwater (Griffioen, 2003), (Eqs. (2) and (3)):

$$\mathrm{i-EXCH} = (\mathrm{i})_{\mathrm{sample}} - (\mathrm{i})_{\mathrm{cons}} \tag{2}$$

and

$$= (\mathrm{i})_{(\mathrm{fresh})} + \left[(\mathrm{i})_{(\mathrm{sea})} - (\mathrm{i})_{(\mathrm{fresh})}\right] * \left[\mathrm{Cl}_{(\mathrm{sample})} - \mathrm{Cl}_{(\mathrm{fresh})}\right] / \left[\mathrm{Cl}_{(\mathrm{sea})} - \mathrm{Cl}_{(\mathrm{fresh})}\right] \tag{3}$$

where i-EXCH (in meq/l) is the degree of exchange for cation i (positive in case of net desorption, and negative in the case of net adsorption), (i) is the equivalent concentration of cation i, and the subscripts 'sample', 'cons', 'fresh' and 'sea' indicate sample, conservative mixing and fresh water and seawater as end-member types, respectively. The degree of exchange was calculated for the cations Na, K, Mg and Ca. The Na-EXCH and Mg-EXCH values may be too sensitive to show spurious cation exchange for saline groundwater due to very high Cl, Na and Mg concentrations and analytical errors in these analyses. Faulty analyses of the water samples can result in spurious cation exchange values (Griffioen, 2003). If the standard deviation of groundwater records is 2%, the probable relative error in the exchange amount will be 2.8% (as denoted as i-EXCH). Accordingly, to avoid including false-positive or false-negative Na-EXCH values, we calculated the probable errors that Na-EXCH should exceed. The probable error for Na^+ in freshwater (Cl < 300 mg/L) is less than 0.1 meq/l. For brackish water (300 < Cl < 5000 mg/L) and saline water (Cl > 5000 mg/L), the probable errors are 0.4 and 1.5 meq/l, respectively. When the degree of Na-EXCH was within the probable error range, the sample was classified as 'No cation exchange' (Table 2). Here, the indications 'late-stage' and 'initial' refer to the preferential order in which Na^+ and Mg^{2+} are exchanged (Appelo and Postma, 2004).

2.5. Handling of probably erroneous data

All groundwater records were collected and processed as described in Section 2.3. Integrating groundwater datasets from multiple sources involves numerous challenges which can be split into two categories: 1) data handling, related to the use of different templates for recording the analysis results (the data needs to be transformed to a single template) and 2) process handling, related to standardising the concentration units, identifying reliable samples, handling the solute concentrations reported below Detection Limit (DL) and removing outlier data. Below, we provide background information on handling non-detect data (i.e., data reported below DL) and detecting outlier data.

2.5.1. Data with multiple DLs

Integrating groundwater quality datasets from various sources obtained over a long period of time also introduces multiple DLs for individual components. Different DLs result from lab technicians applying different analytical methods with varying values of DL and from advances in analytical instrumentation that lead to improved detection limits (McGrory et al., 2020).

Differences and changes in DL values can result in parameters being overestimated or underestimated and can also affect the outlier data

test. Typically, non-detected data (i.e., data reported below DL) in the environmental analysis are removed or substituted (i.e., replaced by a numerical value, e.g., 0 or a factor times DL), leading to values that can be higher or lower than the true value (Farnham et al., 2002; Hansen et al., 2015; Helsel, 2010, 2011). Using these traditional approaches for dealing with non-detected values in datasets can trigger an inaccurate interpretation, especially if the data is heterogeneous. Indeed, many regulatory agencies still have no consistent methodology to handle data below DL. For example, although the US-EPA (the United States Environmental Protection Agency) and EUGD (Europe Groundwater Directive) advocate substituting non-detected concentrations with half the value of the DL (US-EPA, 2000), this substitution is not recommended for handling non-detected pesticides (European Union, 2006). In contrast, Helsel and Hirsch (2010) suggest omitting data below DL. However, omitting data in groundwater analysis is rare, as doing so would result in loss of information.

No information about the procedures for establishing the DLs for the relevant laboratory analyses was available when compiling our database. DLs can be identified using multivariate analyses, such as binary, ordinal and Wilcoxon-type methods. However, these methods have many disadvantages, e.g., a loss of information, the limitation of extracting one single DL and the large time investment involved (McGrory et al., 2020). An alternative standard method for manually identifying detection limits uses scatter charts with sample numbers on the x-axis and the parameter value on the y-axis. Regularly recurring parameter values in the low range are indicative of DLs. A logarithmic scale on the y-axis can facilitate tracing DLs, especially when a parameter ranges over many orders of magnitude.

Our procedure first identified detection limits by drawing scatter plots for the groundwater components (Figure A1 in the Appendix). In accordance with (Grima et al., 2014; Hansen et al., 2015; McGrory et al., 2020), we replaced the identified non-detect entries with the lowest identified DL limit if several DLs limits were identified for a single component (e.g., for NO_3: 1.2 mg/L, 0.5 mg/L, 0.28 mg/L, 0.1 mg/L, 0.05 mg/L, 0.04 mg/L, 0.03 mg/L, 0.02 mg/L, 0.01 mg/L). The non-detect entries were zero if only one DL was identified (e.g., for Fe: 0.02 mg/L).

2.5.2. Data with outliers, spatial autocorrelation and Local Moran index

Median values are robust in statistical water quality data analyses, as single outliers do not influence the analysis. Sampling locations must have at least three samples per screen to calculate medians. A total of 3493 locations did not meet this criterion, and so median values could not be calculated. To identify outlier data, we used an alternative method based on spatial autocorrelation: we compared parameter values for a given screen with values for neighbouring screens and identified potential outliers using the procedure described below.

Global Moran's I index is a correlation coefficient that quantifies whether or not the distribution of a trait among a set of data is affected by the data's spatial relationships. This index expresses whether neighbouring samples are similar, different (positive or negative spatial correlations) or independent of each other (Esri, 2019). The Global Moran's I index is defined as (Wang, 2020) (Equs. 4 and 5):

$$I = \frac{n \times \sum_{i}^{n} \sum_{j}^{n} W_{ij}(x_i - \bar{x})(x_j - \bar{x})}{\sum_{i}^{n} \sum_{j}^{n} W_{ij} \times \sum_{i}^{n} (x_i - \bar{x})^2} \quad (4)$$

$$Z = \frac{\text{Moran's I-E(I)}}{\sqrt{\text{Var}\,(I)}} \quad (5)$$

where n is the number of spatial units indexed by i and j, x is the variable of interest (in this case, ageing indices), and $\bar{x}$ is the average of x. W_{ij} is written in a weight matrix with n by n cells. The spatial weight matrix quantifies spatial neighbourhoods or dependency. This weight matrix summarises the spatial connectivity of the dataset, which is needed for spatial dependency indices like Moran's. The weight matrix can also highlight local clusters where at least two adjacent samples are similar.

In Equation (2), the Z-scores show the significance of the Global Moran's I. E(I) is the expectation value for Moran's I, and Var(I) is the variance of Moran's I. When $Z > 1.96$ and $p < 0.05$, the null hypothesis should be rejected, and spatial autocorrelation should be visible.

Local indicators of spatial association (LISA) have been extensively utilised to assess spatial accumulation and aggregation characteristics. The formula for calculating LISA is (Equ. 6):

$$I_i = Z_i^{'} \sum_{i}^{n} W_{ij} Z_j^{'} \quad (6)$$

where Z_i is a standardised version of the original variable x_i. The LISA coefficient ranges from +1 to −1, and values close to 1 indicate a high degree of similarity among nearby features, which means LISA coefficients are spread out in space and can be used to find clusters of low concentrations (low-low, LL) or high concentrations (high-high, HH). Conversely, a value close to −1 indicates a high dissimilarity among nearby features. Concerning the weight matrix, a high concentration could be surrounded by low ones (HL) or vice versa (LH). Thus, the data points yielding a negative Moran's I index could be outlier data if no median could be calculated per screen. Consequently, potential outlier data revealed by this procedure were discarded from the analysis.

2.5.3. The interpolation method

We found it necessary to utilise an interpolation method that would accurately visualise the defined redox and cation exchange classes. This method's accuracy depends on many factors, including sampling distribution, number of samples and degree of normality (Güler and Kara, 2014; Hengl, 2009; Stahl et al., 2006; Wu et al., 2016). Five interpolation methods have been commonly used in ArcMap to make distribution maps for groundwater quality (Murphy et al., 2010; Güler and Kara 2014), including RBF (Radial basis function), IDW (Inverse Distance Weighting), OK (Ordinary Kriging), LPI (Local Polynomial Interpolation) and EBK (Empirical Bayesian Kriging. When Zaresefat and Derakhshani, 2024recently compared these five interpolation methods for groundwater quality data, such as Fe, Cl, PO_4, NH_4 and SO_4 concentrations, in the same study area, they found the EBK method to be the most accurate based on root mean square analysis values obtained by cross-validation. This method was chosen for its accuracy, among other things. The EBK method offers numerous advantages, specifically in groundwater records analysis. EBK can handle unknowns in model parameters well using different semivariogram models made automatically through subsetting and simulation (Gribov and Krivoruchko, 2020). This functionality facilitates the automatic interpolation of data. Furthermore, the EBK model's ability to make robust predictions even with scarce data is achieved by extrapolating from regional patterns or independently expanding upon these patterns. This capability is precious when sufficient data is unavailable (Krivoruchko, 2012). When dealing with irregular or unusual data collection patterns or disparate data points spanning time and space, the EBK model shows remarkable promise as a practical method to carry out thorough and accurate data analysis (Zaresefat et al., 2023b).

2.6. Spatial Analyst tools and math toolbox

To define the conditional function for identifying hydrogeochemical boundaries (e.g., for redox classes), grid math tools or software with built-in options for enforcing specific property constraints are required. We used Spatial Analyst, an extension in ArcMap that provides a powerful set of mathematical functions to implement or create mathematical relationships, e.g., for managing the output values using conditional functions. In turn, the conditional functions are used to implement high-pass or low-pass filters or to eliminate overlapping

raster cells. These functions allow for applying multiple criteria while retaining the ability to use the remaining raster cells simultaneously. These techniques apply our criteria and manipulate the maps (Tables 1 and 2). The final map indicated the hydrogeochemical boundaries for redox and cation exchange groups.

2.7. Method validation

A comparison was made between the predicted and the observed classes in monitoring wells for all groundwater records to evaluate the method's accuracy. The classes observed for all groundwater records for cation exchange and redox classes were first calculated in Excel and transferred to the ArcMap environment. We then extracted the predicted classes of the redox and cation exchange maps and recorded the values in the attribute table of the monitoring wells for all sampling intervals. If the actual and predicted values were identical for each monitoring well, they were labelled 'YES'; if the values were not identical, they were labelled 'NO'. The similarity percentage was calculated using the total numbers of 'YES' and 'NO' labels.

3. Results and discussion

3.1. Mapping results

The first step in our data pre-processing was the identification of outliers. To deal with the hydrogeological heterogeneity of the study area, we set the distance band in the weight matrix to 3000 m to keep the potential local clusters in the study area. Next, we calculated the Local Moran's I index for Cl, SO_4, Fe, NO_3, Mg-EXCH and Na-EXCH. We discarded detected outliers that did not meet one of the following criteria: 1) at least three samples per screen and 2) at least two similar values surrounding the sample. Table 3 summarises the results from the outlier detection analysis. It shows that the number of outliers was limited, especially compared to the large sample counts. Figure A2 in the Appendix also displays the locations of the outliers for the groundwater components of interest.

Figs. 3 and 4 present the redox and cation exchange maps for all eight depth intervals as prepared with the conditional functions set. Specific areas within the study area boundaries have been interpolated and extrapolated here, which emphasises the need for accuracy and the importance of adopting a geostatistical approach to the study area before applying any overlay. The geostatistical process aids in identifying the most appropriate interpolation method for creating each thematic map.

The detailed interpretation of the maps lies beyond the scope of the present paper, as our objective is to demonstrate our method's intrinsic properties rather than present a geographical interpretation. Fig. 3 shows that all redox classes are present in the areas with local suboxic or mixed groundwater occurrences at more shallow depths (0–15 m). Fig. 4 shows that there is also a large variation in cation exchange classes. The blue, late-stage freshening classes are more prominent at more shallow depths (0–20 m), whereas the reddish, late-stage salinising classes are more prominent at greater depths (30–50 m). This finding is consistent with there being more fresh groundwater at shallow depths and more saline groundwater at larger depths (Post et al., 2003).

3.2. Accuracy of the mapping procedures

Tables 4 and 5 show the results derived from comparing the observed redox status and cation exchange conditions from the groundwater analysis and the geostatistically predicted status at the monitoring well. These results indicate a generally strong agreement between the observed and geostatistically predicted redox status. Overall, the similarity of observations and predictions varies between 88% and 95% with respect to the redox classification, except for the mixed class. Here, the greatest similarities between prediction and observation were for the SO_4 reduced and SO_4 reducing classes: 95% and 92%, respectively. Next came the suboxic class, with 91% similarity. The weakest similarities were observed for the mixed class: between 31 and 85%, with 57% overall. The regional spatial patterns of the predicted redox class are acceptable and correspond with common perceptions about groundwater in the Western Netherlands (e.g. Frapporti et al. (1993); Griffioen et al. (2013)), all of which confirms that the correct method was chosen.

The comparison between observed and predicted classes for the cation exchange state indicates that the 'No cation exchange' similarity varies between 85 and 100%, with an average of 94%, implying that the method reliably identifies the areas with no cation exchange phenomena (Table 5). Overall, the similarity in the cation exchange classification varies between 73% and 81%, except for 'Late-stage of freshening saline water' and 'Initial salinising freshwater', for which the similarity is 65% and 47%, respectively. The poorer similarity between predicted and observed classes in the cation exchange map might be attributable to the presence of more cation exchange classes than redox classes. However, we did not expect to find an exact correlation between the predicted and observed classes in monitoring wells for two main reasons: 1) the uneven spatial distribution of the monitoring wells and 2) the precision of the interpolation methods. One should keep in mind that there are no monitoring screens within the 0–5 m BSL depth in polders because those polders lie several metres BSL, and their uppermost part, consisting of Holocene deposits, is relatively impermeable. Because of the aforementioned points, no screens have been installed in this layer; most observation wells penetrating to 15 m NAP are located in coastal dunes, ice-pushed ridges and wells that penetrate from 15 to 50 m BSL are distributed more evenly throughout the test region.

The number of groundwater records and the dataset's normality are the most important factors affecting the accuracy of interpolation methods (Güler and Kara, 2014; Hengl, 2009; Stahl et al., 2006; Wu et al., 2016). Cation exchange patterns have not been mapped at a regional scale for the Western Netherlands, but the regional patterns we observed are logical given where the intrusion of seawater (diluted or undiluted) is likely to predominate over the infiltration of fresh rain, river or lake water. One can therefore conclude that the chosen mapping method provides useful results.

Table 3
The number of outliers determined using the Local Moran's I indices for the eight depth layers. HL refers to a high concentration surrounded by low ones, and HL refers to a low concentration surrounded by high ones.

Depth layers (m - NAP)	Cl			SO_4			Fe			NO_3			Mg-EXCH			Na-EXCH		
	Count	HL	LH	Count	HL	LH	Count	HL	LH	Count	HL	LH	Count	HL	LH	Count	HL	LH
0 to 5	249	0	2	253	0	2	247	2	0	249	1	2	249	2	0	249	1	1
5 to 10	359	0	0	360	0	0	355	0	0	352	0	1	360	2	2	360	3	2
10 to 15	451	1	3	455	0	0	452	1	0	448	2	1	455	0	0	455	0	0
15 to 20	463	0	1	462	0	0	458	0	4	454	0	0	462	1	2	462	0	0
20 to 25	519	0	3	519	0	0	511	2	6	509	0	0	519	0	1	519	0	0
25 to 30	485	1	2	485	1	1	484	0	3	479	0	0	485	0	3	485	0	0
30 to 40	503	1	0	503	0	0	502	1	1	489	6	3	503	4	0	503	2	0
40 to 50	317	2	0	317	0	2	315	0	2	306	5	0	317	0	0	317	0	0

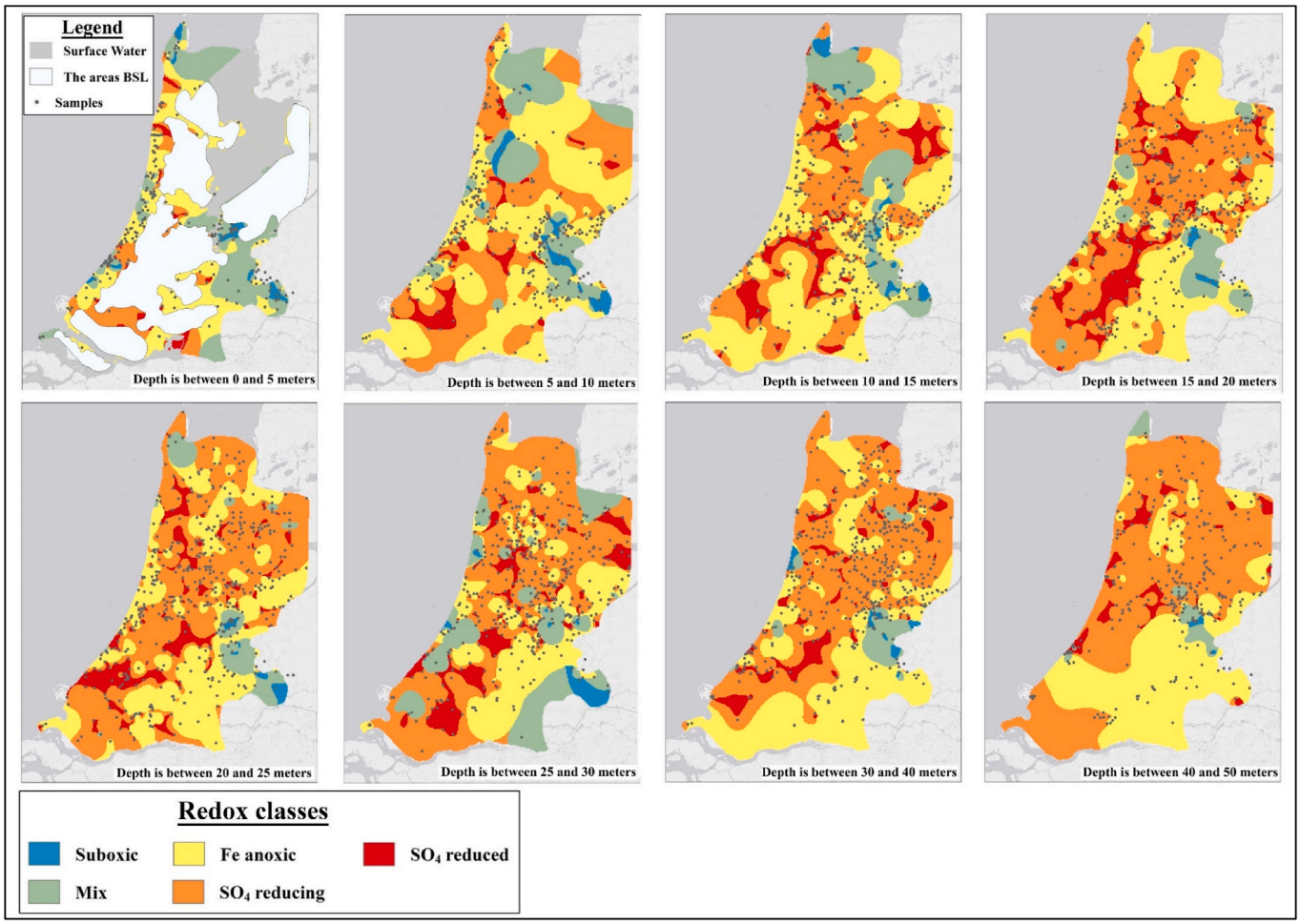

Fig. 3. Redox classification maps for groundwater in the Western Netherlands. Much of the study area lies below sea level, which leads to few groundwater observation wells at 0–5 m NAP outside the dunes and ice-pushed ridge.

3.3. Pros and cons of the method

Our findings demonstrate the efficiency and user-friendly nature of this novel GIS method for mapping non-numerical groundwater quality information on a regional scale. While alternative methods like machine learning (ML) offer advantages, those methods require user input and continuous model improvement (Zaresefat et al., 2023a; Zaresefat and Derakhshani, 2023). In contrast, the presented method offers a simpler and more readily applicable approach.

The method leveraged the flexibility of the Math Toolbox in ArcGIS to classify groundwater composition efficiently (Lukman, 2021) based on redox status and cation exchange conditions. To achieve efficient classification, we combined readily available raster layers with functions like overlay, conditional and combination statements. Although user-defined pixel size affects how spatial features are linked, our chosen method was much faster and more accurate when working with large datasets (Netzel and Slopek, 2021). Consequently, due to this improved efficiency and user-friendliness, the presented GIS method offers a valuable alternative for mapping non-numerical groundwater quality data.

However, the limitations of the GIS method must be acknowledged. Unlike ML, which utilises model-based spatial structures to minimise errors and better capture spatial trends, this method relies on predefined rules and relationships between data points. Such a dependence can limit effectiveness in capturing complex spatial variations or unforeseen patterns. Therefore, consideration of our method's limitations (including the lack of model-based spatial structure incorporation) is critical in order to make the best choice for the most suitable approach for specific projects.

4. Conclusions

This study has established a GIS method to map the redox and cation exchange states as important aspects of groundwater quality, where these states are the result of the classification procedure. The method was tested using a dataset from the Western Netherlands. Mapping both aspects was found to provide useful results regarding spatial patterns and similarity between observed and predicted classes. The method's primary benefit is its mathematically or programmatically geostatistical model-based approach, which incorporates the data's spatial structures, thereby minimising errors and reproducing spatial trends. One innovative aspect of our method includes using the raster calculator in ArcMap to generate non-numerical classifications and facilitate complex spatial data calculations. The method uses the power and flexibility of mathematical tools in a GIS system to classify various spatial properties, such as groundwater attributes, based on multiple variables. The method presented can also be applied to map other non-numerical multivariate spatial characteristics, providing valuable insights into the quality and suitability of groundwater for various uses in different parts of the world.

Funding

No funding was obtained for this study.

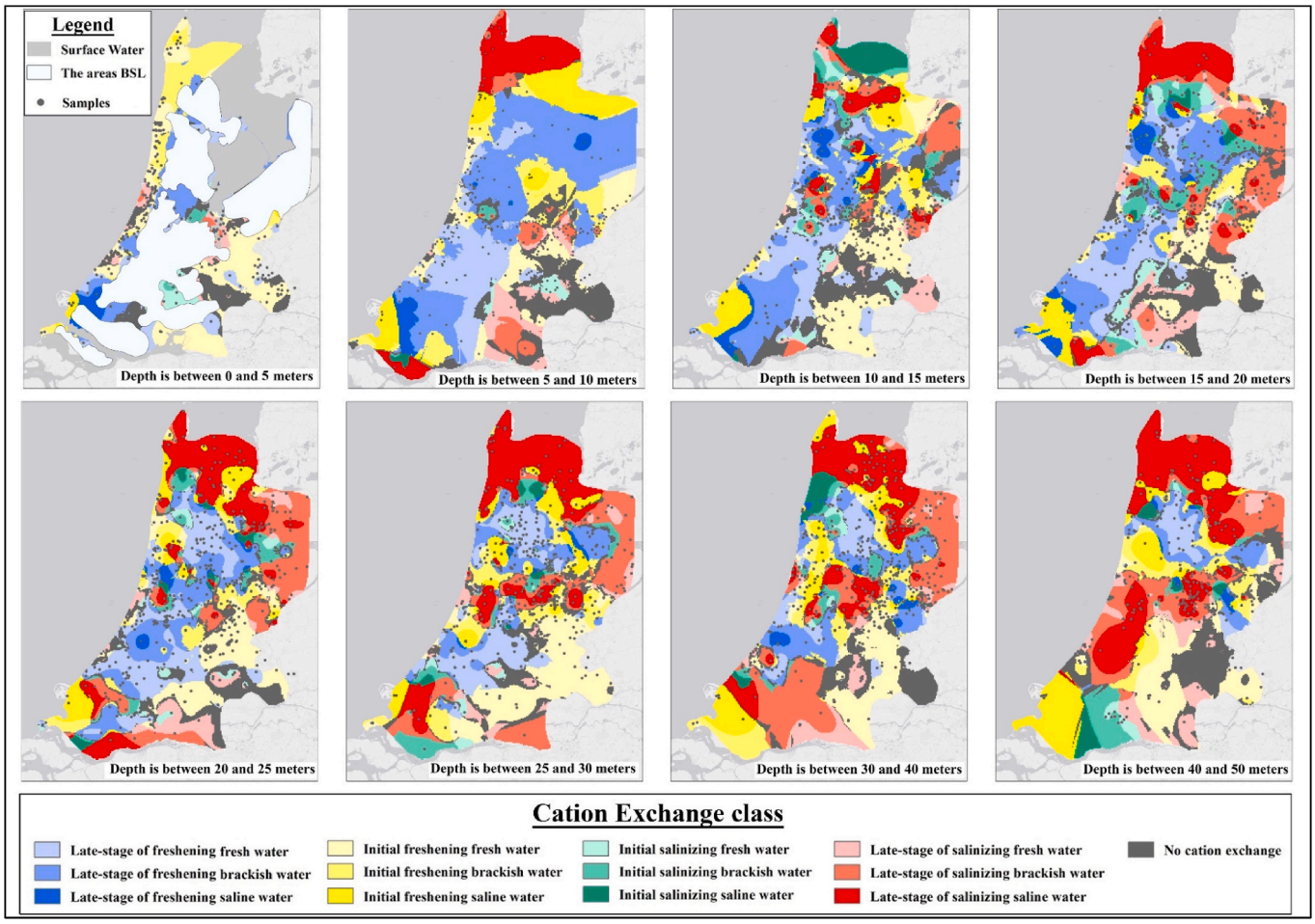

Fig. 4. Cation exchange classification maps for groundwater in the Western Netherlands.

Table 4
Similarity between the redox status observed from the groundwater analysis and the geostatistically predicted redox class. Percentage Accuracy (PA) refers to the proportion, and Number of Screens (NS) refers to the count of monitoring wells.

Redox status	Validation	Depth interval layers (m BSL)								Overall
		0 to 5	5 to 10	10 to 15	15 to 20	20 to 25	25 to 30	30 to 40	40 to 50	
Suboxic	NS	36	20	16	10	10	6	13	6	117
	PA	89%	85%	100%	90%	100%	100%	85%	83%	91%
Mixed	NS	39	23	17	13	15	27	13	11	158
	PA	49%	52%	47%	85%	53%	74%	31%	64%	57%
Fe anoxic	NS	115	172	186	140	158	123	146	80	1120
	PA	91%	94%	89%	86%	90%	89%	85%	81%	88%
SO_4 reducing	NS	39	117	162	222	254	228	286	198	1506
	PA	87%	85%	93%	95%	92%	95%	94%	94%	92%
SO_4 reduced	NS	18	24	67	74	77	99	43	17	419
	PA	100%	100%	93%	92%	99%	90%	91%	94%	95%

Availability of data and material

The primary data are freely available from the DINO database of the TNO Geological Survey of the Netherlands. The GIS scripts could be available upon request.

Ethical approval

All authors have read, understood, and complied as applicable with the statement on 'Ethical responsibilities of Authors' as found in the Instructions for Authors. Additionally, all authors are aware that, with minor exceptions, no changes can be made to authorship once the paper is submitted.

CRediT authorship contribution statement

Walter Schenkeveld: Writing – review & editing, Validation, Supervision, Resources, Project administration.

Declaration of competing interest

The authors declare the following financial interests/personal relationships which may be considered as potential competing interests: Mojtaba Zaresefat reports article publishing charges was provided by

Table 5
Comparison between the cation exchange conditions observed from the groundwater analysis and the geostatistically predicted class. Percentage Accuracy (PA) refers to the proportion, and Number of Screens (NS) refers to the count of monitoring wells.

Cation exchange conditions	Validation	Depth interval layers (m BSL)								Overall
		0 to 5	5 to 10	10 to 15	15 to 20	20 to 25	25 to 30	30 to 40	40 to 50	
Late-stage freshening fresh water	NS	27	67	74	79	112	89	53	28	529
	PA	85%	72%	68%	78%	84%	91%	83%	82%	80%
Late-stage freshening brackish water	NS	9	39	55	35	52	58	47	17	312
	PA	67%	62%	73%	71%	87%	79%	83%	82%	75%
Late-stage freshening saline water	NS	1	5	8	9	10	2	8	5	48
	PA	100%	60%	50%	44%	70%	100%	38%	60%	65%
Initial freshening fresh water	NS	92	67	68	44	66	56	58	28	479
	PA	75%	48%	74%	82%	82%	88%	71%	82%	75%
Initial freshening brackish water	NS	19	16	21	43	35	48	43	21	246
	PA	47%	69%	62%	79%	83%	79%	77%	81%	75%
Initial freshening saline water	NS	6	12	17	16	15	19	36	12	133
	PA	100%	58%	41%	69%	67%	84%	81%	83%	73%
No cation exchange	NS	15	38	47	41	26	26	35	19	247
	PA	93%	95%	94%	95%	85%	92%	94%	100%	94%
Initial salinising fresh water	NS	5	13	16	14	13	10	9	7	87
	PA	40%	69%	38%	50%	15%	30%	67%	57%	46%
Initial salinising brackish water	NS	4	1	13	23	17	14	18	7	97
	PA	100%	100%	62%	43%	76%	86%	94%	86%	81%
Initial salinising saline water	NS	No data		2	7	10	7	6	4	36
	PA	No data		50%	86%	80%	86%	100%	100%	84%
Late-stage salinising fresh water	NS	35	32	19	41	20	23	29	31	230
	PA	51%	31%	42%	54%	80%	65%	45%	65%	54%
Late-stage salinising brackish water	NS	6	22	28	40	35	34	63	26	254
	PA	67%	45%	68%	63%	77%	74%	84%	62%	67%
Late-stage salinising saline water	NS	8	20	24	26	56	53	66	83	336
	PA	50%	70%	75%	81%	95%	89%	92%	83%	79%

Utrecht University. Mojtaba Zaresefat reports a relationship with Utrecht University that includes.

Data availability

Data will be made available on request.

Acknowledgements

This research is part of a PhD project by the first author, Mojtaba Zaresefat, who would like to express his sincere gratitude for the financial support from the I.R. Iran government's scholarship programme, funded by the Ministry of Science, Research and Technology (MSRT). Joy Burrough and Adam Frick are gratefully acknowledged for providing linguistic advice. Finally, the paper's two anonymous reviewers are thanked for their constructive feedback.

Appendix A. Supplementary data

Supplementary data to this article can be found online at https://doi.org/10.1016/j.gsd.2024.101188.

References

Amini, M.A., Torkan, G., Eslamian, S., Zareian, M.J., Adamowski, J.F., 2019. Analysis of deterministic and geostatistical interpolation techniques for mapping meteorological variables at large watershed scales. Acta Geophysica 67. https://doi.org/10.1007/s11600-018-0226-y.

Appelo, C.A.J., Postma, D., 2004. Geochemistry, groundwater and pollution, geochemistry. Groundwater and Pollution, second ed. CRC Press, Rotterdam. https://doi.org/10.1201/9781439833544.

Appelo, C.A.J., Willemsen, A., 1987. Geochemical calculations and observations on salt water intrusions, I. A combined geochemical/minxing cell model. J. Hydrol. (Amst.) 94, 313–330. https://doi.org/10.1016/0022-1694(87)90058-8.

Beekman, H.E., 1991. Ion Chromatography of Fresh- and Seawater Intrusion: Multicomponent Dispersive and Diffusive Transport in Groundwater (PhD Thesis). Vrije Universiteit, Amsterdam.

Brindha, K., Taie Semiromi, M., Boumaiza, L., Mukherjee, S., 2023. Comparing Deterministic and Stochastic Methods in Geospatial Analysis of Groundwater Fluoride Concentration. Water (Switzerland) 15. https://doi.org/10.3390/w15091707.

Christensen, T.H., Bjerg, P.L., Banwart, S.A., Jakobsen, R., Heron, G., Albrechtsen, H.J., 2000. Characterization of redox conditions in groundwater contaminant plumes. J. Contam. Hydrol. https://doi.org/10.1016/S0169-7722(00)00109-1.

CLO, 2021. Compendium for the Living environment [WWW Document]. URL. https://www.clo.nl/indicatoren/nl0004-meteorologische-gegevens-in–nederland, 1.19.22.

Close, M.E., Abraham, P., Humphries, B., Lilburne, L., Cuthill, T., Wilson, S., 2016. Predicting groundwater redox status on a regional scale using linear discriminant analysis. J. Contam. Hydrol. 191, 19–32. https://doi.org/10.1016/J.JCONHYD.2016.04.006.

Drever, J., 1997. Redox conditions in natural waters. In: The Geochemistry of Natural Waters: Surface and Groundwater Environments.

Dufour, F., 2000. Groundwater in the Netherlands: Facts and Figures. Netherlands Institute of Applied Geoscience TNO, Delf, The Netherlands.

Ehteshami, M., Salari, M., Zaresefat, M., 2016. Sustainable development analyses to evaluate groundwater quality and quantity management. Model Earth Syst Environ 2. https://doi.org/10.1007/s40808-016-0196-5.

Esri, 2019. ArcGIS geostatistical Analyst | model spatial data & uncertainty [WWW Document]. URL. https://www.esri.com/en-us/arcgis/products/geostatistical-analyst/overview.

European Union, 2006. Directive 2006/118/EC of the European Parliament and of the council of 12 December 2006 on the protection of groundwater against pollution and deterioration. Off. J. Eur. Union 19.

Farnham, I.M., Singh, A.K., Stetzenbach, K.J., Johannesson, K.H., 2002. Treatment of nondetects in multivariate analysis of groundwater geochemistry data. Chemometr. Intell. Lab. Syst. 60, 265–281. https://doi.org/10.1016/S0169-7439(01)00201-5.

Frapporti, G., Vriend, S.P., van Gaans, P.F.M., 1993. Hydrogeochemistry of the shallow Dutch groundwater: interpretation of the national groundwater quality monitoring Network. Water Resour. Res. 29, 2993–3004. https://doi.org/10.1029/93WR00970.

Friedel, M.J., Wilson, S.R., Close, M.E., Buscema, M., Abraham, P., Banasiak, L., 2020. Comparison of four learning-based methods for predicting groundwater redox status. J. Hydrol. (Amst.) 580, 124200. https://doi.org/10.1016/j.jhydrol.2019.124200.

Gribov, A., Krivoruchko, K., 2020. Empirical Bayesian kriging implementation and usage. Sci. Total Environ. 722, 137290 https://doi.org/10.1016/j.scitotenv.2020.137290.

Griffioen, J., 2003. Kation-uitwisselingspatronen bij zoet/zout grondwaterverplaatsingen. Stromingen 9, 35–45.

Griffioen, J., 1994. Uptake of Phosphate by iron Hydroxides during seepage in relation to development of groundwater composition in coastal areas. Environ. Sci. Technol. 28, 675–681. https://doi.org/10.1021/ES00053A022.

Griffioen, J., Passier, H.F., Klein, J., 2008. Comparison of selection methods to deduce natural background levels for groundwater units. Environ. Sci. Technol. 42, 4863–4869. https://doi.org/10.1021/es7032586.

Griffioen, J., Vermooten, S., Janssen, G., 2013. Geochemical and palaeohydrological controls on the composition of shallow groundwater in The Netherlands. Appl. Geochem. 39, 129–149. https://doi.org/10.1016/j.apgeochem.2013.10.005.

Grima, J., Luque-Espinar, J.A., Mejía-Gómez, J.Á., Rodríguez, R., 2014. Analysis of Groundwater Monitoring Data Sets with Non-Detect Observations: Application to the

Plana de Sagunto (Valencia, Spain) Groundwater Body. Lecture Notes in Earth System Sciences 507–512. https://doi.org/10.1007/978-3-642-32408-6_111, 0.
Güler, M., Kara, T., 2014. Comparison of different interpolation techniques for modelling temperatures in middle black sea region. Agric. Fac. Gaziosmanpasa Univ 31, 61–71. https://doi.org/10.13002/jafag714.
Hansen, C.T., Ritz, C., Gerhard, D., Jensen, J.E., Streibig, J.C., 2015. Re-evaluation of groundwater monitoring data for glyphosate and bentazone by taking detection limits into account. Sci. Total Environ. 536, 68–71. https://doi.org/10.1016/J.SCITOTENV.2015.07.047.
Helsel, D., 2011. Statistics for Censored Environmental Data Using Minitab and R. John Wiley & Sons. https://doi.org/10.1002/9781118162729.
Helsel, D., 2010. Much ado about next to nothing: incorporating non detects in science. Ann. Occup. Hyg. 54, 257–262. https://doi.org/10.1093/ANNHYG/MEP092.
Helsel, D., Hirsch, R., 2010. Statistical methods in water resources. Techniques of Water Resources Investigations Book 4. United States Geological Survey, p. 552. Chapter A3.
Hengl, T., 2009. A Practical Guide to Geostatistical Mapping, EUR 22904 EN Scientific and Technical Research Series. Office for Official Publications of the European Communities, Luxembourg.
Karimzadeh Motlagh, Z., Derakhshani, R., Sayadi, M.H., 2023. Groundwater vulnerability assessment in central Iran: integration of GIS-based DRASTIC model and a machine learning approach. Groundw Sustain Dev 23. https://doi.org/10.1016/j.gsd.2023.101037.
Krivoruchko, K., 2012. Empirical bayesian kriging. ArcUser Fall 6, 1145.
Lall, U., Josset, L., Russo, T., 2020. A snapshot of the world's groundwater challenges. Annu. Rev. Environ. Resour. 45, 171–194. https://doi.org/10.1146/annurev-environ-102017-025800.
Lukman, M.N., 2021. Using raster calculator in QGIS GUI and Python console to make SR blocks [WWW Document]. URL. https://nasirlukman.github.io/2021-08-08-Raster-Calculator/.
Luo, Y., Guo, W., Ngo, H.H., Nghiem, L.D., Hai, F.I., Zhang, J., Liang, S., Wang, X.C., 2014. A review on the occurrence of micropollutants in the aquatic environment and their fate and removal during wastewater treatment. Sci. Total Environ. https://doi.org/10.1016/j.scitotenv.2013.12.065.
McGrory, E., Holian, E., Morrison, L., 2020. Assessment of groundwater processes using censored data analysis incorporating non-detect chemical, physical, and biological data. J. Contam. Hydrol. 235, 103706 https://doi.org/10.1016/J.JCONHYD.2020.103706.
Mu, L., 2009. Thiessen polygon. International Encyclopedia of Human Geography II, 231–236. https://doi.org/10.1016/B978-008044910-4.00545-9.
Murphy, R.R., Curriero, F.C., Ball, W.P., 2010. Comparison of spatial interpolation methods for water quality evaluation in the Chesapeake Bay. Environmental Engineering 136, 160–171. https://doi.org/10.1061/(ASCE)EE.1943-7870.0000121.
Naus, F.L., Schot, P.P., Ahmed, K., Griffioen, J., 2019. Groundwater salinity variation in Upazila Assasuni (southwestern Bangladesh), as steered by surface clay layer thickness, relative elevation and present-day land use. Hydrol. Earth Syst. Sci. 23, 1431–1451. https://doi.org/10.5194/hess-23-1431-2019.
Netzel, P., Slopek, J., 2021. Comparison of different implementations of a raster map calculator. Comput. Geosci. 154, 104824 https://doi.org/10.1016/J.CAGEO.2021.104824.
Parkhurst, D.L., Appelo, C.A.J., 1999. User's Guide to PHREEQC (Version 2): A Computer Program for Speciation, Batch-Reaction, One-Dimensional Transport, and Inverse Geochemical Calculations, Water-Resources Investigations Report 99-4259. Denver, Colorado, USA.
Pit, I.R., Egmond, E.M. van, Dekker, S.C., Griffioen, J., Wassen, M.J., Wezel, A.P. van, 2018. Ecotoxicological risk of trace element mobility in coastal semiartificial depositional areas near the mouth of the river Rhine, The Netherlands. Environ. Toxicol. Chem. 37, 2933–2946. https://doi.org/10.1002/ETC.4262.
Post, V.E.A., Van der Plicht, H., Meijer, H.A.J., 2003. The origin of brackish and saline groundwater in the coastal area of The Netherlands. Geologie en Mijnbouw/Netherlands Journal of Geosciences 82, 133–147. https://doi.org/10.1017/S0016774600020692.
Søndergaard, M., 2009. Redox potential. Encyclopedia of Inland Waters. https://doi.org/10.1016/b978-012370626-3.00115-0.
Stahl, K., Moore, R.D., Floyer, J.A., Asplin, M.G., McKendry, I.G., 2006. Comparison of approaches for spatial interpolation of daily air temperature in a large region with complex topography and highly variable station density. Agric. For. Meteorol. 139, 224–236. https://doi.org/10.1016/j.agrformet.2006.07.004.
Stuyfzand, P.J., 2008. Base exchange indices as indicators of salinization or freshening of (coastal) aquifers. In: 20th Salt Water Intrusion Meeting. Naples, Florida, USA.
United States Environmental Protection Agency, 2000. Guidance for Data Quality Assessment. Practical Methods for Data Analysis. Office of Environmental Information. EPA QA/G9. QA00 UPDATE.
Van Den Brink, C., Frapporti, G., Griffioen, J., Zaadnoordijk, W.J., 2007. Statistical analysis of anthropogenic versus geochemical-controlled differences in groundwater composition in The Netherlands. J. Hydrol. (Amst.) 336, 470–480. https://doi.org/10.1016/j.jhydrol.2007.01.024.
Van Geel, B., Brinkkemper, O., Weeda, E.J., Sevink, J., 2017. Formation, vegetation succession and acidification of a Mid-Holocene moorland pool in the western Netherlands. Geologie en Mijnbouw/Netherlands Journal of Geosciences 96. https://doi.org/10.1017/njg.2016.1.
Wang, S., 2020. Spatial patterns and social-economic influential factors of population aging: a global assessment from 1990 to 2010. Soc. Sci. Med. 253, 112963 https://doi.org/10.1016/J.SOCSCIMED.2020.112963.
Weerts, H., Schokker, J., Rijsdijk, K., Laban, C., 2006. Geologische overzichtskaart van Nederland/Geological map of The Netherlands. TNO Built Environment and Geosciences - Geological Survey of the Netherlands (Utrecht, NL).
Wilson, S.R., Close, M.E., Abraham, P., 2018. Applying linear discriminant analysis to predict groundwater redox conditions conducive to denitrification. J. Hydrol. (Amst.) 556, 611–624. https://doi.org/10.1016/J.JHYDROL.2017.11.045.
Wolters, T., Bach, T., Eisele, M., Eschenbach, W., Kunkel, R., McNamara, I., Well, R., Wendland, F., 2022. The derivation of denitrification conditions in groundwater: combined method approach and application for Germany. Ecol Indic 144, 109564. https://doi.org/10.1016/J.ECOLIND.2022.109564.
Wu, W., Tang, X.-P., Ma, X.-Q., Liu, H.-B., 2016. A comparison of spatial interpolation methods for soil temperature over a complex topographical region. Theor. Appl. Climatol. 125, 657–667. https://doi.org/10.1007/s00704-015-1531-x.
Zaresefat, M., Derakhshani, R., 2023. Revolutionizing groundwater management with hybrid ai models: a practical review. Water 2023 15. https://doi.org/10.3390/W15091750, 1750 15, 1750.
Zaresefat, M., Derakhshani, R., Nikpeyman, V., GhasemiNejad, A., Raoof, A., 2023a. Using artificial intelligence to identify suitable artificial groundwater recharge areas for the iranshahr basin. Water 2023 15. https://doi.org/10.3390/W15061182. Page 1182 15, 1182.
Zaresefat, M., Hosseini, S., Roudi, M.A., 2023b. Addressing nitrate contamination in groundwater: the importance of spatial and temporal understandings and interpolation methods. Water 2023 15. https://doi.org/10.3390/W15244220. Page 4220 15, 4220.
Zaresefat, M., Derakhshani, R., 2024. Griffioen, J. Empirical Bayesian Kriging, a straightforward and robust method of spatial data interpolation for groundwater quality analyses from the Western Netherlands. Water submitted for publication.